Sigma J Eng Nat Sci, Vol. 44, No. 5, pp. 3383–3392, October, 2026

Sigma Journal of Engineering and Natural Sciences
Web page info: https://sigma.yildiz.edu.tr
DOI: 10.14744/sigma.2026.2164

Research Article

Numerical investigation of viscoelastic fluid flows past a circular bluff body

Anas AL-HABOOBI[1,*], Alaa H. AL-MUSLIMAWI[2]

[1]*Department of Mathematics, Faculty of Computer Sciences and Mathematics, University of Kufa, Kufa, 54003, Iraq*
[2]*Department of Mathematics, College of Sciences, University of Basrah, Basrah, 61001, Iraq*

ARTICLE INFO

Article history
Received: 19 January 2025
Revised: 05 May 2025
Accepted: 15 June 2025

Keywords:
Drag Coefficient; Incompressible Flow; Isothermal Flow; Oldroyd-B Model; Taylor-Galerkin/Pressure-Correction Method; Viscoelastic Flow

ABSTRACT

This study concerns incompressible viscoelastic fluid flows around bluff bodies, which are special cases of computational rheology, as it has been difficult to deal with this kind of fluid. A new numerical scheme is presented which is an improvement of the Taylor–Galerkin/Pressure-Correction finite element method for simulation of flows of viscoelastic fluids. In this case, the transient flow in an axisymmetric rectangular channel with a circular bluff body is considered. Results are presented to show the importance of two important dimensionless quantities in viscoelastic fluids, namely the solvent fraction and the Weissenberg number, on important aspects of the flow. The results observe that under various settings of solvent fraction and the Weissenberg number excellent agreement with those of previous studies. Moreover, we observed that the drag coefficient obtained for such flow is in good agreement with literature data for such flow. Further, the method was also able to be applied with good performance to higher values of the Weissenberg number where many conventional methods were not successful because of numerical instabilities. All the results we got are consistent physically and also predict well, which is what we want. The novelty of the work is the extension of applicability of the Taylor-Galerkin/Pressure-Correction method to a class of viscoelastic problems that were not previously applicable because of numerical difficulties. The contribution goes beyond the mere development of the computational skills, it also contributes to the understanding of the viscoelastic flow phenomena, particularly for the case of geometric shapes with embedded bluff bodies.

Cite this article as: Al-Haboobi A, Al-Muslimawi AH. Numerical investigation of viscoelastic fluid flows past a circular bluff body. Sigma J Eng Nat Sci 2026;44(5):3383–3392.

INTRODUCTION

The flow past bluff bodies is a classical but challenging problem in fluid dynamics because of the complex fluid characteristics such as boundary layer separation, pressure distribution, drag force fluctuations and vortex shedding. These properties have become very important in engineering applications like heat exchangers, polymer extrusion, aerospace design and biological applications.

***Corresponding author.**
*E-mail address: anasm.ali@uokufa.edu.iq

This paper was recommended for publication in revised form by Editor-in-Chief Ahmet Selim Dalkilic

Published by Yıldız Technical University Press, İstanbul, Turkey
© Author. This is an open access article under the CC BY-NC license (http://creativecommons.org/licenses/by-nc/4.0/).

If the working fluid has non-Newtonian or viscoelastic characteristics, such as polymer solutions and synthetic slurries [1], the basic physics becomes even more complicated. Such flows have been treated in the past by various numerical techniques for understanding and control of wake dynamics and drag behavior. Chiba and Horikawa [2] investigated the influence of shear thinning and elasticity on the flow around a circular cylinder by solving the problems by finite difference method with the perturbation method. Numerical simulations to study two-dimensional steady flows of a viscoelastic fluid past a circular cylinder confined by two parallel walls was used by Huang and Feng [3]. The experimental results of a flow in a rectangular channel with 20 mm width and 0.16 m depth are described, which was used in the finite element package by Verhelst and Nieuwstadt [4]. Şahin and Atalık's [5] interest is related to the parametrical study and comparison of various non-Newtonian phenomena of a circular cylinder in the periodic vortex shedding regime. By adopted the Peterlin approximation, Peng et al. [6] understand the two-dimensional flows past two side-by-side circular cylinders of the finitely extensible nonlinear elastic model.

There are still unanswered questions regarding the above efforts. In the past, most studies have been dedicated to Newtonian fluids and simplified non-Newtonian fluids, while ignoring the computational problems that can arise due to the viscoelastic effects, particularly near bluff bodies. In addition, low Reynolds (*Re*) number simulations with high resolution in order to calculate the complete stress tensor are limited. Such instability problems may be a serious problem for numerical schemes, particularly at high Weissenberg numbers (We), thus restricting their usability in practical applications.

To overcome this, in this study, a powerful and efficient numerical method, named as Taylor-Galerkin/Pressure-Correction (TG/PC) finite element method, originally developed by Hawken and Tamaddon-Jahromi [7] is used. Various extensions of the application of TG/PC scheme are given that show its particular suitability in order to solve problems involving numerical instabilities for viscoelastic flow models like Oldroyd-B as well as for fluid problems in general. Tamaddon-Jahromi et al. [8] investigate the proper type of the Taylor/Galerkin based algorithms to accurately solve the model convection - diffusion problems in time. Carew et al. [9] have adopted their uesd TG/PC method to solve the problem of viscoelastic flow through a 4:1 planar contraction. TG/PC method was uesd to solve problems that manifest free surfaces associated with the incompressible creeping flow of Newtonian fluids by Ngamaramvaranggul and Webster [10]. Al-Muslimawi [11] uesd TG/PC to find numerical predictions of die-swell flow for viscoelastic and viscoelastoplastic fluids. Using the TG/PC method Sharhan and Al-Muslimawi [12] performed a numerical study on inelastic fluid flow with different shear properties flowing through axisymmetric contractions with various contraction ratios. Al-Haboobi and Al-Muslimawi [13] developed non-isothermal model for solving fluid problem using TG/PC. Al-Haboobi et al. used the TG/PC method to simulate the incompressible flow [14] and compressible flow [15] around bluff bodies under isothermal conditions. In the present work, this approach is used to simulate Poiseuille flow in an axisymmetric channel with a circular bluff body, and the flow parameters of drag coefficient (D_c), pressure (p), normal stress components (τ_{zz}) and the first and second normal stress differences (N_1 and N_2) are presented as functions of β and We.

The novelty of this work is due to three main contributions: First, it offers a high accuracy simulation of the flow of viscoelastic fluids past a bluff body at low Reynolds number, where many of the traditional methods are not applicable because of their numerical instability. Second, it provides an in-depth parametric study which quantifies the effect of viscoelastic properties on force and stress measurements. Third, the numerical method is converged and reliable, so it can be applied in other industries when meeting the following requirements: industrial or biomedical industry, the equipment has a similar physical property as that simulated in the research. The results are a major improvement in the computational modelling of non-Newtonian flows.

New advances in so-called 'nanofluids', which are fluids containing nano-sized particles, have also recently been found to be of merit for enhancing the properties of heat transfer and fluid transport for complex geometries. The recent studies on the flow behavior of nanofluids in thermal gradient condition, magnetic field condition and porous media condition have shown that the thermal performance and stability of nanofluids have improved [16-23]. In other flow regimes (e.g., microfluidics) where solar collectors or electronic cooling systems are involved, the use of nanofluid technology in a viscoelastic or non-Newtonian environment might offer other methods to enhance the ability to control flow around the bluff. The methodology and the gained insights in this study serve as a good foundation for further studies with advanced working fluids (nanofluids and hybrid materials) for the further extension of the range of applicability of non-Newtonian flow modelling and prediction capability. Moreover, the current configuration may be extended to the more complicated geometries, such as three-dimensional bluff bodies, which can be used to describe the flow behaviour of viscoelastic fluids in more realistic engineering configurations. In section 2, the mathematical modeling of non-Newtonian isothermal flow and its non-dimensional form are presented. The TG/PC finite element methodology is detailed in Section 3. The effect of viscoelastic parameters on flow characteristics is highlighted in Sections 4 and 5, giving the problem set-up and numerical results respectively.

MATHEMATICAL MODELING

The non dimensional form of the equations governing flow of an incompressible viscoelastic fluid in cylindrical coordinates is [24-26]:

$$\nabla \cdot u = 0. \tag{1}$$

$$Re\frac{\partial u}{\partial t} = -\nabla p + \beta\nabla\cdot(\nabla u + (\nabla u)^T) + \nabla\cdot\tau - Re(u\cdot\nabla)u. \tag{2}$$

$$We\frac{\partial \tau}{\partial t} = (1-\beta)(\nabla u + (\nabla u)^T) - \tau - \mathrm{We}\big((u\cdot\nabla)\tau - (\tau\cdot\nabla u + (\nabla u)^T\cdot\tau)\big). \tag{3}$$

This makes the above three equations the equations of continuity, momentum and stress, respectively. In this, u is velocity, p is pressure and τ is stress, respectively. In addition, the definition of the Reynolds number, Weissenberg number and the part of the solvent is given as [13, 14, 25]:

$$Re = \frac{\rho U_\infty L}{\mu},$$
$$We = \frac{\lambda U_\infty}{L},$$
$$\beta = \frac{\mu_s}{\mu}.$$

Here, U_∞ is the characteristic velocity, L is the characteristic length, ρ is the density, μ_s is the viscosity of the solvent and μ is the total viscosity ($\mu = \mu_s + \mu_e$). Also, λ represents relaxation time.

Numerical Method

One of the very efficient numerical methods was used in this study, and produced extremely accurate results in the field of fluid mechanics, known as a Taylor-Galerkin/Pressure-Correction scheme (TG/PC). This scheme results in a time stepping scheme to solve the non-linear coupled mode equation in the finite element setting. The governing equations are discussed here by considering a three-step computation per time-step of the (TG/PC). Since this approach is employed based on the finite element method, so the non-dimensional differential equations (1)-(3) are transformed into a system of linear equations, and then use an iterative method to find the final numerical solutions. For the velocity calculations an efficient element by element Jacobi technique was used, while for the pressure step a direct Cholesky decomposition method was used. The temporal derivative is extended by the finite difference method (FDM) and the spatial component is converted by the weighted residual technique of the classic Galerkin finite element method (FEM). The partial differential equations (4)-(9):

Step 1a:

$$u^{n+1/2} = u^n + \frac{\Delta t}{2Re}(L(u^n,\tau^n) - \nabla p^n), \tag{4}$$

$$\tau^{n+1/2} = \tau^n + \frac{\Delta t}{2We}F(u^n,\tau^n), \tag{5}$$

Step 1b:

$$u^* = u^n + \frac{\Delta t}{Re}\big(L\big(u^{n+1/2},\tau^{n+1/2}\big) - \nabla p^n\big), \tag{6}$$

$$\tau^{n+1} = \tau^n + \frac{\Delta t}{2We}F\big(u^{n+1/2},\tau^{n+1/2}\big), \tag{7}$$

Step 2:

$$\nabla^2(p^{n+1} - p^n) = \frac{Re}{\Delta t}\nabla\cdot u^*, \tag{8}$$

Step 3:

$$u^{n+1} = u^* - \frac{\Delta t}{Re}\nabla(p^{n+1} - p^n). \tag{9}$$

Where,

$$L(u,\tau) = \beta\nabla\cdot(\nabla u + (\nabla u)^T) + \nabla\cdot\tau - Re(u\cdot\nabla)u,$$

$$F(u,\tau) = (1-\beta)(\nabla u + (\nabla u)^T) - \tau - We\big((u\cdot\nabla)\tau - (\tau\cdot\nabla u + (\nabla u)^T\cdot\tau)\big).$$

The Jacobi iterative method is used to approximate step 1a, 1b, and 3, and the Cholesky decomposition scheme is used to determine step 2. In order to stabilize the approximate solution, the local velocity gradient recovery and streamline-upwind Petrov/Galerkin procedures are utilized after this step has been completed.

Problem Specification and Boundary Conditions

The study focuses on a viscous, incompressible fluid flow through a channel containing a circular body within the flow domain. The channel has a length of 10 units and a height of 5 units. The finite element mesh used in this problem consists of 1,953 elements, 1,050 vertices, and 13,356 degrees of freedom (Fig. 1). To run the simulation, the boundary conditions are considered as Poiseuille flow at the inlet of the channel and no-slip boundary conditions at the top wall of the channel and around the circular bluff body. At the outlet of the channel, zero radial velocity and

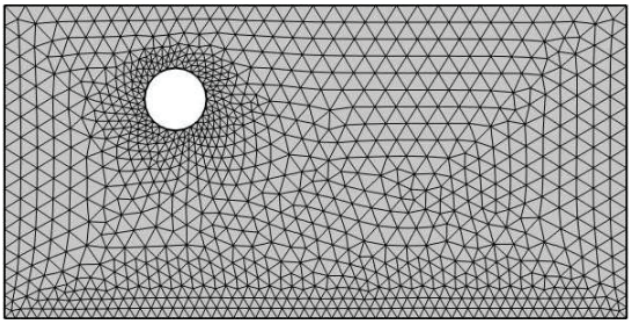

Figure 1. Computing mesh.

pressure are enforced. For the stress equation at the inlet, we define the stresses τ_{zz} and τ_{rz} according to the following analytical expressions [25]:

$$\tau_{zz} = 8We(1-\beta)((u_z)_{max}r/h)^2,$$
$$\tau_{rz} = -2(1-\beta)((u_z)_{max}r/h).$$

RESULTS

We addressed the problem using (TG/PC). To meet the research objectives, we investigated the influence of the Weissenberg number (*We*) and viscosity (β) on pressure (p), normal stress (τ_{zz}), the first and second normal stresses (N_1 and N_2), strain-rates (Σ) and shear-rates (Γ). The results obtained will demonstrate the efficiency of this method in solving the problem and reveal the impact of the bluff body on the viscoelastic fluid. The Reynolds number *Re* was held low at 10^{-4} throughout the analysis.

The drag coefficient, $C_d = \frac{d}{0.5\rho\, U^2\, A}$, is a dimensionless quantity that quantifies the resistance, or drag force, encountered by an object as it moves through a fluid, such as air or water. This coefficient is a key factor in fluid dynamics and aerodynamics, serving as a critical tool for modeling and analyzing the drag force one of the primary forces that oppose the motion of objects through a fluid. Given its significance in the analysis of bluff bodies, we begin by examining the influence of β= (0.01,0.05,0.1) on the drag coefficient, particularly in relation to variations in the Weissenberg number (*We*). As depicted in Figure 2, an increase in the Weissenberg number corresponds to a decrease in the drag coefficient. Furthermore, for different values of β, it is evident that larger values of β result in a more pronounced impact on the drag coefficient, as noted in [27].

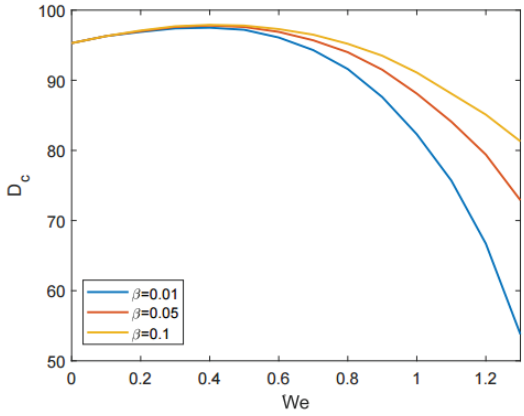

Figure 2. The drag coefficient.

***β*-Variation** The parameter β is very important to understand the role of the solvent in the overall viscosity of the viscoelastic fluid [28]. An investigation was carried out along the centreline of the channel to gain insight into the influence on the parameters τ_{zz}, N_1 and N_2 of the channel parameter β, which was varied with the values 0.01, 0.1 and 0.9. In Figure 3 the influence of β on the value of τ_{zz} is discussed. From Figure 3(a) it can be seen that a decrease in β value corresponds to a significant growth in $\tau_{zzvalue}$, this can be explained by the shear-thinning effect mentioned in [29]. The influence of solvent-fraction β on $\tau_{zzalong}$ the cylinder surface is shown in Figure 3(b) for the various values of β: 0.9, 0.1 and 0.01, and for a fixed value of We=1. The results show that the shear-thinning behaviors have great influence on the decrease of τ_{zzas} the level of β increases. For example, the profile of gives an increase in normal stress of O(92\%) from β = 0.9 to β = 0.01, O(90\%) from β = 0.8 to β = 0.1. While there was a slight increase in τ_{zz} of around O(10\%) from β= 0.1 to β = 0.01. Practically, the increase in normal stress on the cylinder surface can be understood as due to the interactions between the fluid and the solid surface resulting from the increase in level of viscosity.

The effect of changing the value of the β parameter is shown in Figure 4, both for N_1 and N_2. For each, it is

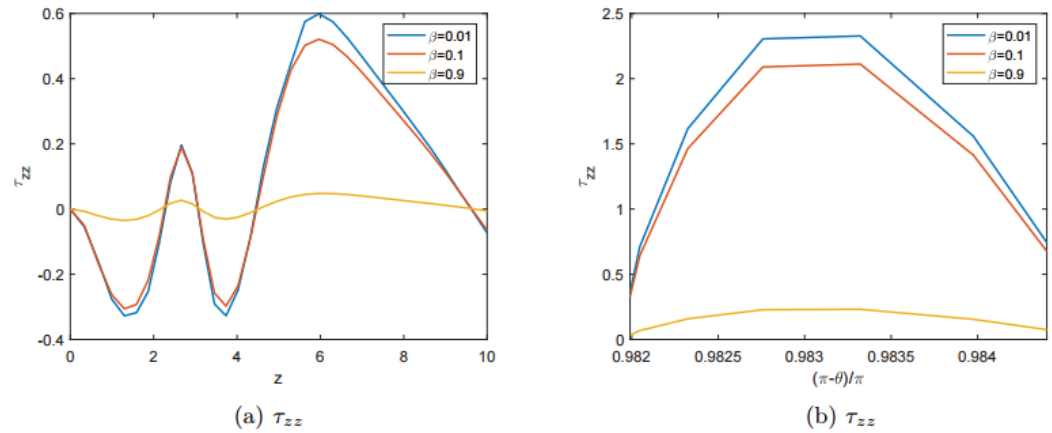

(a) τ_{zz} (b) τ_{zz}

Figure 3. Effect of β on τ_{zz}.

seen that as the value of the β decreases, its respective level increases greatly. It is interesting to note that the increase for N_1 is larger than for N_2 because the solvent exhibits viscous behaviour compared to the elastic behaviour of the polymer [29].

As far as the effects of the bluff body, it's clear that there is a huge difference in the level of τ_{zz}, N_1 and N_2 starting at the point of the bluff body's inception. This is mostly due to the effect of flow separation [14].

***We*-Variation**

Weissenberg number is an important parameter in the study of viscoelastic fluid such that ratio of the elastic forces to the viscous forces. It represents the recoverable strain in the fluid, and thus is important to understand the fluid behaviour [30]. The effect of *We* on p, τ_{zz}, N_1 and N_2 is studied for three different values of β. The pressure distributions on the cylinder are shown in Figure 5. The upstream pressures increase as the We increases, while the base

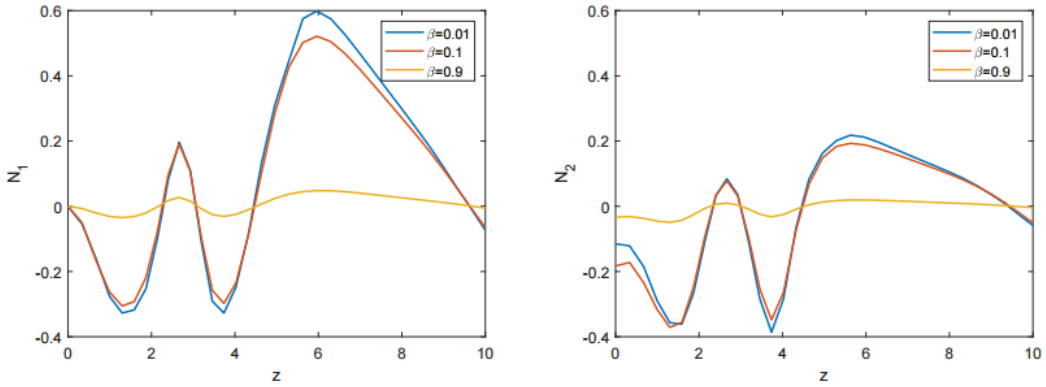

(a) N_1 (b) N_2

Figure 4. Effect of β on (a) N_1 and (b) N_2.

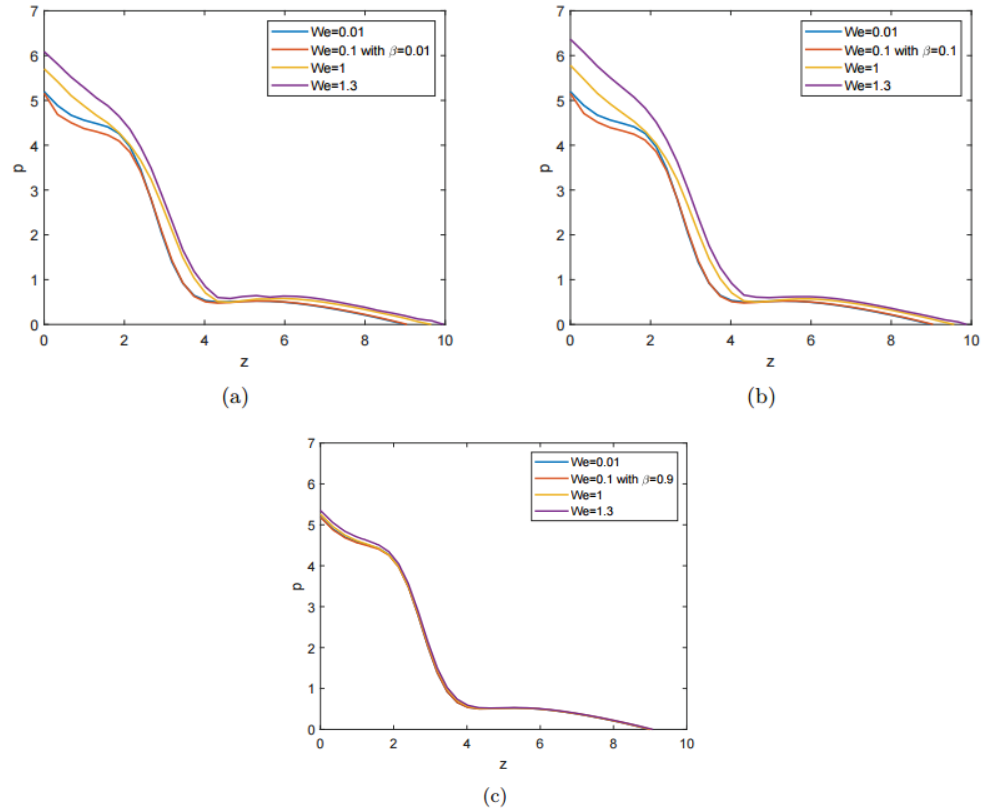

(a) (b)

(c)

Figure 5. Effect of *We* on pressure with different value of β.

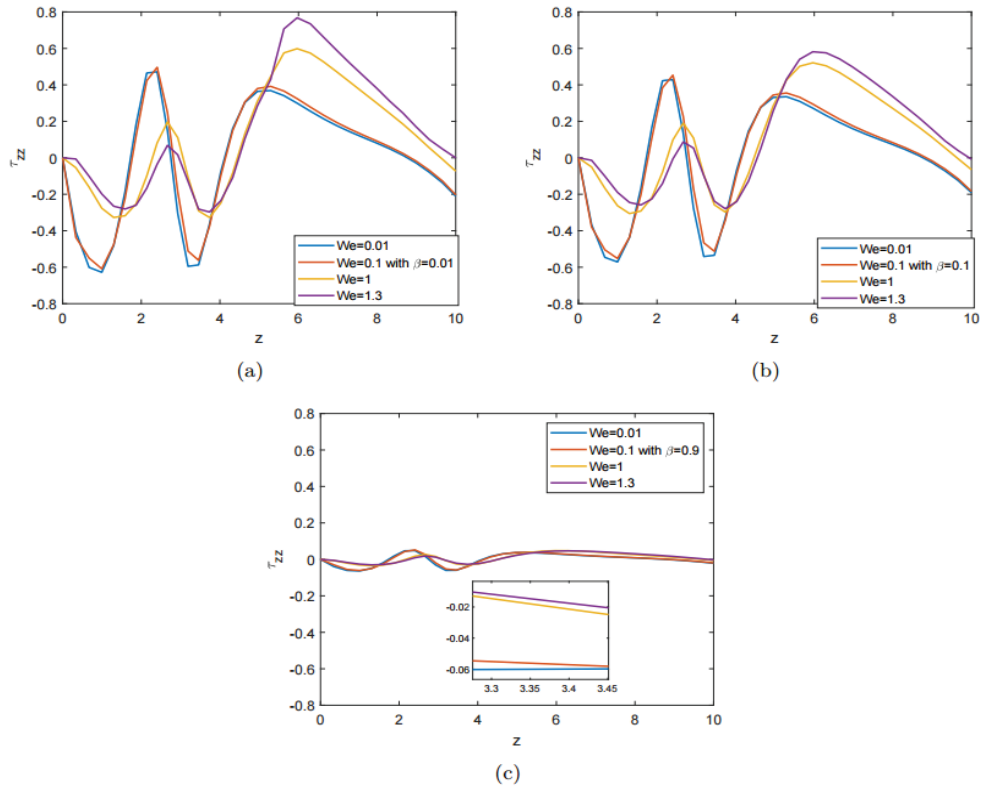

Figure 6. Effect of *We* on τ_{zz} with different value of β.

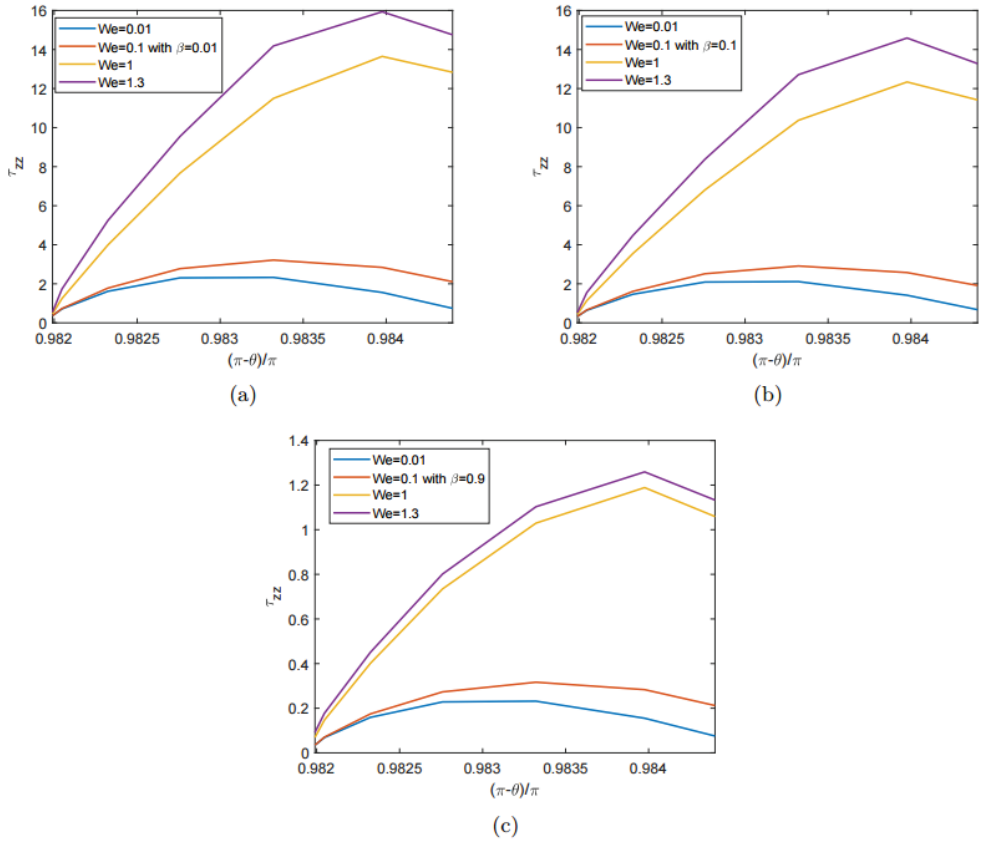

Figure 7. Effect of *We* on τ_{zz} distributions with different value of β of cylinder surface.

pressure at the downstream end of the cylinder shows the opposite behavior. At high Weissenberg numbers the additional stagnation pressure and reduced base pressure cause the cylinder to experience more drag. The drag does not vary significantly at low We, nor is there any measurable change in pressure. The base pressure in the downstream zone shows a rebound after a short distance, followed by a short high base pressure. At the end of the cylinder, the pressure decreases gradually, caused by the pressure drop in the conduit. The pressure is restored to zero at the outlet and thus, the reference pressure is set in the computational domain. If the value of β is reduced, there will be a greater effect on We.

The effect of *We* on the normal stress component τ_{zz} is illustrated in Figure 6. It is evident that increasing *We* leads to a significant increase in τ_{zz},with the effect being more pronounced at lower values of β. Additionally, Figure 6 shows the influence of the bluff circular body on the

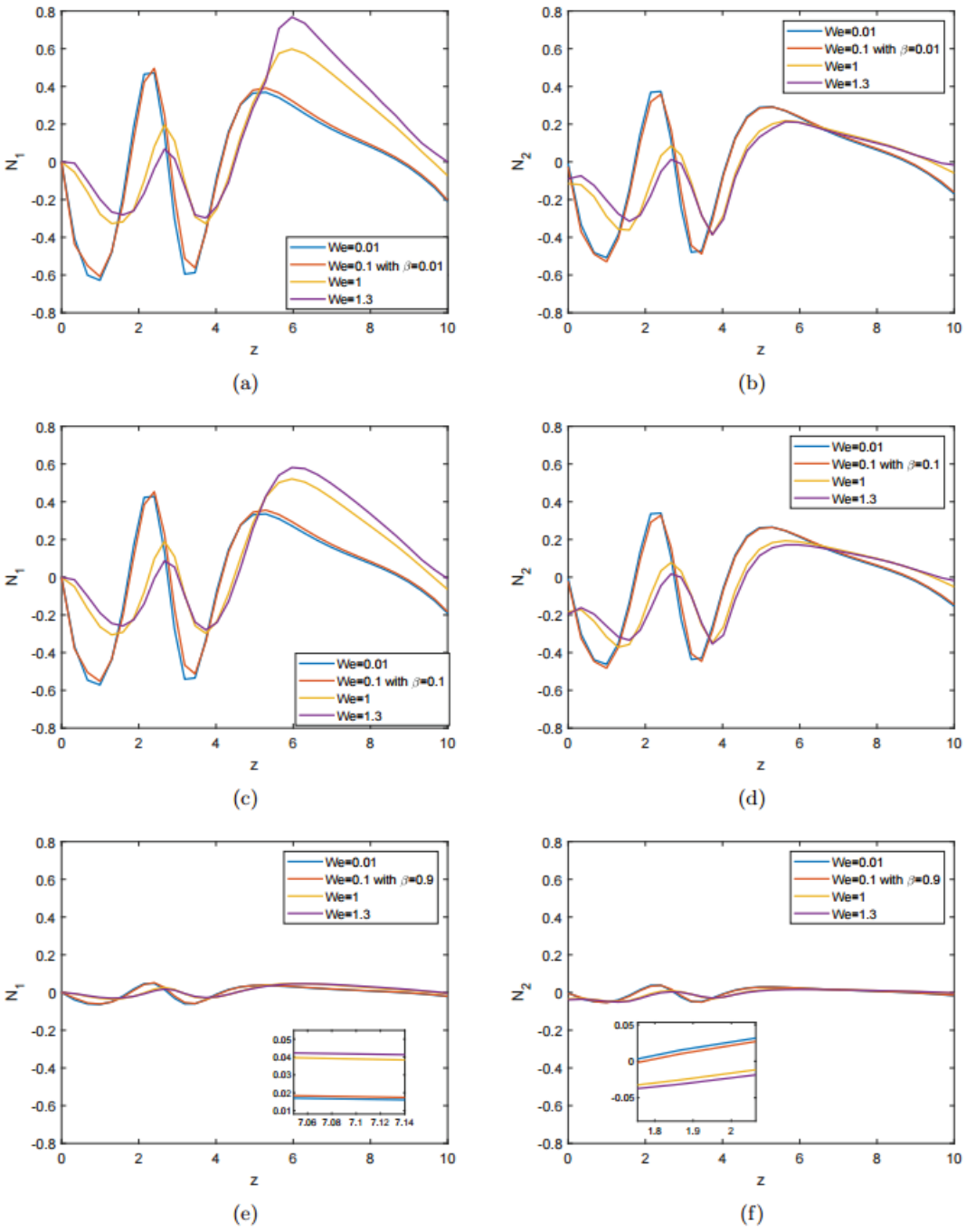

Figure 8. Comparison of the effect of *We* on N_1 and N_2 with different value of β.

distribution of τ_{zz}. At the location of the body, τ_{zz} is notably altered, but it returns to its typical rising pattern after the fluid passes around the body.

Figure 7 gives a clear feature of the effect of the Weissenberg number (We) and solvent-fraction (β) on normal stress around cylinder surface. This figure is plotted with the same setting of parameters. The profiles reflect many facts, the first of which is the observed impact of β on the level of τ_{zz} in this region, as there is a significant increase in the level of τ_{zz} when β decreases. In addition, the influence of shear-thinning behaviour is also clearly shown by the increase in τ_{zz} as the We -value increases.

Ultimately, we present the effect of We on both the first N_1 and second N_2 normal stress differences, comparing their respective impacts, as illustrated in Figure 8. Before drawing comparisons, we observe that the effect of We on N_1 is entirely analogous to its effect on τ_{zz}, as evident in Figures 8(a, c, e) and Figure 6. This similarity arises because τ_{rr} is zero at the channel centerline. Given the definition $N_1 = \tau_{zz} - \tau_{rr}$, it follows that $N_1 = \tau_{zz}$, resulting in identical effects and

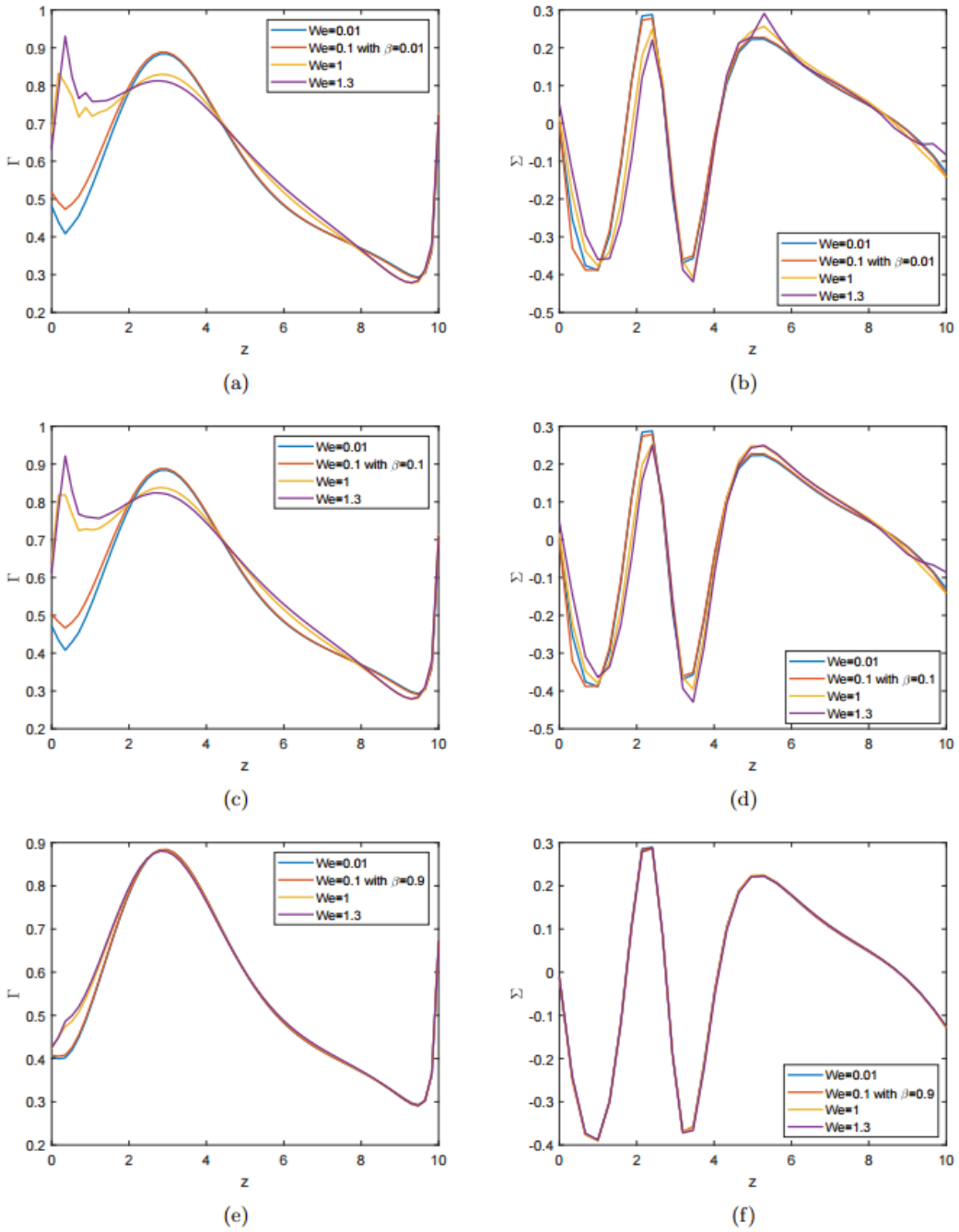

Figure 9. Comparison of the effect of We on Γ and Σ with different value of β.

behavior for both N_1 and τ_{zz}. Figure 9, displays the influence of *We* on strain-rates (Σ) and shear-rates (Γ) on the centerline and top wall, respectively, under three β-value = {0.9,0.1,0.01}. The profiles show that, insignificant effect from β is occurred on strain-rates and shear-rates due to the nature of Oldroyd-B model. In the cases of elasticity effects on strain-rates and shear-rates, one can observe very little change in the level of stresses, with modest increasing with decreases *We*. The modest effect of *We* may be due to the fact that the solutions were with small values of *We*, as high values of the *We* were not reached because of the complexity of this type of problem. In this context, the critical level of *We* was 1.3, Which is a natural issue with Oldroyd-B model. In addition, the maximum level of Γ is almost three times greater than the Σ level due to the domination of shear in this type of fluid. Moreover, results reflect that there is overshoot near the cylinder surface in the shear-rates, whilst in the train-rates we observed overshoot then undershoot in succession, which reflects the effect of interactions between the fluid and the solid surface. Returning to the discussion on the effect of the Weissenberg number (*We*) on both the first (N_1) and second (N_2) normal stress differences, Figure 8 demonstrates that as *We* increases, N_1 increases correspondingly. In contrast, the range of N_2 decreases as *We* increases. Additionally, we observe that these effects are more pronounced at lower values of β.

Regarding the effect of the bluff circular body on the distribution of both N_1 and N_2, at the location of the body, N_1 and N_2 are notably altered. However, they return to their typical rising patterns after the fluid passes around the body. All results presented were consistent with the findings reported in [14, 27, 29].

CONCLUSION

This study presented a comprehensive numerical investigation of incompressible viscoelastic fluid flow around a circular bluff body using a novel and efficient Taylor-Galerkin/Pressure-Correction (TG/PC) finite element method. We investigated systematically the influence of important parameters on the critical flow characteristics at a low Reynolds number ($Re = 10^{-4}$): the viscosity ratio, the Weissenberg number, the drag coefficient, pressure distribution, normal stress components and normal stress differences. The results show that the pressure and normal stresses increase with increasing Weissenberg number and the first and second normal stress differences decrease with increasing viscosity ratio. The following observations highlight the interplay between the elastic and viscous effects in viscoelastic flows. In quantitative terms, the Taylor-Galerkin/Pressure-Correction method gave excellent accuracy in comparison with the available benchmarks, and was also found to be very stable in the numerical treatment of the flow even at high Weissenberg number, where many of the established schemes are susceptible. More importantly, it was observed that the geometry of a bluff body plays a significant role in the flow structure and the distribution of stresses, thus motivating the need for ensuring accurate geometric modelling for practical applications. The results have immediate applications in various industrial and biomedical applications such as polymer processing, modelling of blood flow in vessels containing obstructions, and methods of reducing drag in fluid-structure interactions. The proposed approach for the simulation of complex viscoelastic phenomena, namely the Taylor-Galerkin/Pressure-Correction method approach, leads to new avenues to reliably simulate complex viscoelastic phenomena in geometrically complex domains.

AUTHORSHIP CONTRIBUTIONS

Authors equally contributed to this work.

DATA AVAILABILITY STATEMENT

The authors confirm that the data that supports the findings of this study are available within the article. Raw data that support the finding of this study are available from the corresponding author, upon reasonable request.

CONFLICT OF INTEREST

The authors declared no potential conflicts of interest with respect to the research, authorship, and/or publication of this article.

ETHICS

There are no ethical issues with the publication of this manuscript.

STATEMENT ON THE USE OF ARTIFICIAL INTELLIGENCE

Artificial intelligence was not used in the preparation of the article.

REFERENCES

[1] Chhabra RP, Richardson JF. Non-Newtonian flow in the process industries: fundamentals and engineering applications. Oxford, UK: Butterworth-Heinemann; 1999.

[2] Chiba K, Horikawa A. Numerical solution for the flow of viscoelastic fluids around an inclined circular cylinder. I. The flow around a circular cylinder. Rheol Acta 1987;26:243–254. [CrossRef]

[3] Huang PY, Feng J. Wall effects on the flow of viscoelastic fluids around a circular cylinder. J Non-Newtonian Fluid Mech 1995;60:179–198. [CrossRef]

[4] Verhelst JM, Nieuwstadt FTM. Visco-elastic flow past circular cylinders mounted in a channel: experimental measurements of velocity and drag. J Non-Newtonian Fluid Mech 2004;116:301–328. [CrossRef]

[5] Şahin A, Atalık K. Comparison of inelastic and elastic non-Newtonian effects on the flow around a circular cylinder in periodic vortex shedding. J Non-Newtonian Fluid Mech 2019;263:1–14. [CrossRef]
[6] Peng S, Xiong YL, Xu XY, Yu P. Numerical study of unsteady viscoelastic flow past two side-by-side circular cylinders. Phys Fluids 2020;32. [CrossRef]
[7] Hawken DM, Tamaddon-Jahromi HR, Townsend P, Webster MF. A Taylor-Galerkin-based algorithm for viscous incompressible flow. Int J Numer Methods Fluids 1990;10:327–351. [CrossRef]
[8] Tamaddon-Jahromi HR, Ding D, Webster MF, Townsend P. A Taylor-Galerkin finite element method for non-Newtonian flows. Int J Numer Methods Eng 1992;34:741–757. [CrossRef]
[9] Carew EOA, Townsend P, Webster MF. A Taylor-Petrov-Galerkin algorithm for viscoelastic flow. J Non-Newtonian Fluid Mech 1993;50:253–287. [CrossRef]
[10] Ngamaramvaranggul V, Webster MF. Computation of free surface flows with a Taylor-Galerkin/pressure-correction algorithm. Int J Numer Methods Fluids 2000;33:993–1026. [CrossRef]
[11] Al-Muslimawi AH. Theoretical and numerical studies of die swell flow. Korea Aust Rheol J 2016;28:229–236. [CrossRef]
[12] Sharhan A, Al-Muslimawi A. Inelastic solution for power law fluid with Taylor-Galerkin/pressure-correction finite element method: axisymmetric contraction flows. J Appl Fluid Mech 2023;16:2411–2423. [CrossRef]
[13] Al-Haboobi A, Al-Muslimawi AH. Novel algorithm for compressible Newtonian axisymmetric thermal flow. Int J Mod Phys C 2024;35:1–11. [CrossRef]
[14] Al-Haboobi A, Al-Juaifri GA, Al-Muslimawi AH. Numerical study of Newtonian laminar flow around circular and square cylinders. Results Control Optim 2024;14:100328. [CrossRef]
[15] Al-Haboobi A, Fadhel IA, Sharhan AA, Al-Muslimawi AH. Computational simulation of compressible Newtonian flow past circular and square bluff bodies. Ocean Syst Eng 2024;14:315–330. [CrossRef]
[16] Pati AK, Mishra S, Misra A, Mishra SK. Heat and mass transport aspects of nanofluid flow towards a vertical flat surface influenced by electrified nanoparticles and electric Reynolds number. East Eur J Phys 2024;2024:234–241. [CrossRef]
[17] Pati AK, Rout MM, Sahu R, Ramakoti IS, Panda KK, Sethi KC. Chemical reaction, electrification, Brownian motion and thermophoresis effects of copper nanoparticles on nanofluid flow with skin friction, heat and mass transfer. East Eur J Phys 2024;2024:152–158. [CrossRef]
[18] Mishra S, Pati AK, Misra A, Mishra SK. Thermal performance of nanofluid flow along an isothermal vertical plate with velocity, thermal, and concentration slip boundary conditions employing Buongiorno's revised non-homogeneous model. East Eur J Phys 2024;2024:98–106. [CrossRef]
[19] Pati AK, Misra A, Mishra SK. Effect of electrification of nanoparticles on heat and mass transfer in boundary layer flow of a copper-water nanofluid over a stretching cylinder with viscous dissipation. JP J Heat Mass Transf 2019;17:97–117. [CrossRef]
[20] Pati AK, Misra A, Mishra SK, Mishra S, Sahu R, Panda S. Computational modelling of heat and mass transfer optimization in copper-water nanofluid flow with nanoparticle ionization. JP J Heat Mass Transf 2023;31:1–18. [CrossRef]
[21] Thirupathi G, Govardhan K, Nagaraju G, Misra S. MHD upper-convected Maxwell hybrid nanofluid over a stretching sheet: a numerical approach. Sigma J Eng Nat Sci 2025;43:429–440. [CrossRef]
[22] Akaje TW, Olajuwon BI, Raji MT. Computational analysis of the heat and mass transfer in a Casson nanofluid with a variable inclined magnetic field. Sigma J Eng Nat Sci 2023;41:512–523. [CrossRef]
[23] Ghule VM, Pawar AA, Patil LN, Javanjal VK. Numerical and experimental investigation of cross cut angle impact on heat transfer in microchannels. Sigma J Eng Nat Sci 2025;43:463–486. [CrossRef]
[24] Lukaszewicz G, Kalita P. Navier-Stokes equations. Vol. 34. Springer; 2016. [CrossRef]
[25] Fadhel IA, Al-Muslimawi AH. Simulation of Oldroyd-B viscoelastic fluid in axisymmetric straight channel by using a hybrid finite element/volume method. J Adv Res Fluid Mech Therm Sci 2021;81:26–40. [CrossRef]
[26] Bayraktar S. Laminar flow over sloped downstream heated bottom wall behind a backward-facing step. Sigma J Eng Nat Sci 2020;38:1555–1566.
[27] Phan-Thien N, Dou HS. Viscoelastic flow past a cylinder: drag coefficient. Comput Methods Appl Mech Eng 1999;180:243–266. [CrossRef]
[28] Larson RG. The structure and rheology of complex fluids. Vol. 150. Oxford University Press; 1999.
[29] Al-Muslimawi AH. Numerical study for differential constitutive equations with polymer melts by using a hybrid finite-element/volume method. J Comput Appl Math 2016;308:488–498. [CrossRef]
[30] White JL. Dynamics of viscoelastic fluids, melt fracture, and the rheology of fiber spinning. J Appl Polym Sci 1964;8:2339–2357. [CrossRef]